Sub-barrier fusion of $^{36}S + ^{64}Ni$ and other medium-light systems

G. Montagnoli,[1] A. M. Stefanini,[2] L. Corradi,[2] S. Courtin,[3] E. Fioretto,[2] F. Haas,[3] D. Lebhertz,[3] F. Scarlassara,[1] R. Silvestri,[2] and S. Szilner[4]

[1]*Dipartimento di Fisica, Università di Padova, and INFN, Sezione di Padova, I-35131 Padova, Italy*
[2]*INFN, Laboratori Nazionali di Legnaro, I-35020 Legnaro (Padova), Italy*
[3]*IPHC, CNRS-IN2P3, Université Louis Pasteur, F-67037 Strasbourg Cedex 2, France*
[4]*Ruđer Bošković Institute, HR-10002 Zagreb, Croatia*

(Received 2 October 2010; published 23 December 2010)

Sub-barrier fusion cross sections of $^{36}S + ^{64}Ni$ have been measured down to $\simeq 3$ μb. The logarithmic slope of the fusion excitation function has a steep rise in the barrier region with decreasing energy and saturates at lower energies. The data can be reproduced within the coupled-channels model using a Woods-Saxon potential with a large diffuseness. The slope saturation is analogous to what has been observed for ^{36}S, $^{48}Ca + ^{48}Ca$, while for heavier systems the slope increases steadily below the barrier.

DOI: 10.1103/PhysRevC.82.064609 PACS number(s): 25.70.Jj, 24.10.Eq

I. INTRODUCTION

Heavy-ion fusion cross sections in the energy region near the Coulomb barrier result from a balance of several concurring effects. Some of these enhance the fusion probability (couplings to internal degrees of freedom of the colliding nuclei and to nucleon transfer channels), whereas others cause a limitation to fusion (competition with deep inelastic or quasi-fission channels) especially for heavy and/or symmetric systems. A further type of limitation has been reported in recent years in the deep sub-barrier region where experimental fusion cross sections systematically fall below the predictions of standard coupled-channels (CC) calculations. This phenomenon is known as "fusion hindrance" and is commonly represented by using the logarithmic derivative (slope) $L(E) = d\ln(E\sigma)/dE$ which is very sensitive to the trend of the excitation function at very low energies.

This fusion hindrance has first been observed in $^{60}Ni + ^{89}Y$ [1] and later on in several other cases [2–6]. It was suggested that it is a general phenomenon of heavy-ion interaction at far sub-barrier energies [2] (see also the systematics of Ref. [3]). For medium-mass systems the slopes, below the barrier, reach and overcome the value L_{CS} expected for a constant astrophysical S factor $S(E)$ [4,7], implying the presence of a maximum of $S(E)$ as a function of the energy. For instance, this was observed for $^{58}Ni + ^{58}Ni$ [8], $^{64}Ni + ^{64}Ni$ [9], and for the lighter system $^{28}Si + ^{64}Ni$ [10]. The crossing of L_{CS} or, equivalently, a maximum of $S(E)$, was associated to the onset of hindrance. However, the hindrance observed in recent experimental studies of medium-light systems [11,12] was not strong enough to generate a maximum of $S(E)$ in the measured energy range.

Mişicu and Esbensen [13,14] suggested that a shallow pocket of the ion-ion potential develops inside the barrier, due to the saturation properties of nuclear matter. Thus, the barrier is thicker than with standard potentials of Woods-Saxon type [15] and fusion cross sections are smaller. Good fits were obtained for the excitation function of $^{58}Ni + ^{58}Ni$ and $^{64}Ni + ^{64}Ni$ at deep sub-barrier energies. On the other hand, the same data have been successfully reproduced by describing the low-energy compound nucleus (CN) formation as a two-step process, that is, capture in the two-body potential pocket followed by penetration of an adiabatic one-body potential [16,17]. The concept of "decoherence" [5,18] has been also applied to the case of $^{16}O + ^{208}Pb$ low-energy fusion. Measuring fusion cross sections smaller than $\simeq$10–20 nb seems to be necessary to discriminate between these different models.

The energy threshold for hindrance appears to be related to structural properties of the colliding nuclei. In spite of extensive theoretical and experimental systematic work on a broad mass range, basic questions are still pending. For example, in light systems such as various $C + C$ and $O + O$ cases with positive Q values for CN formation, $L(E)$ and L_{CS} are nearly parallel at low energies, and no clear evidence of a maximum in the S factor shows up. Medium-mass systems with $Q > 0$ (where both colliding nuclei have masses in the range $A \simeq 30$–60) have been the object of various recent studies. The possible role played by a positive Q value in the behavior of the excitation function at far sub-barrier energies [2] has been studied since a reliable extrapolation of this role for light systems would be of great astrophysical interest.

Recent data exist for $^{28}Si + ^{30}Si$ (having $Q = +14.3$ MeV) [19] and, in particular, for $^{27}Al + ^{45}Sc$ (having $Q = +9.63$ MeV), where fusion hindrance has been reported [20]. The excitation function was measured to cross sections as low as 300 nb, but this was still not sufficient to reveal a clear maximum in the S-factor representation. Nevertheless, experimental cross sections are smaller than standard CC predictions at low energies, confirming the occurrence of fusion hindrance in that system with positive Q value. The two cases $^{36}S + ^{48}Ca$ [21] and $^{48}Ca + ^{48}Ca$ [12] with Q values of +7.55 MeV and –3 MeV, respectively, were also studied. The structure of the colliding nuclei is similar (very stiff and neutron rich), and the trend of the two excitation functions is very similar, since in both cases the logarithmic slopes saturate below the L_{CS} value. It follows that no significant effect can be attributed to the sign of the Q value.

In this framework, we have decided to study the system $^{36}S + ^{64}Ni$, with a heavier and softer target (^{64}Ni) with respect to the cases cited above. Our aim has been twofold, i.e., to

 ©2010 The American Physical Society

verify if a fusion hindrance is observed in this system, and whether this is associated with a maximum of the S factor as a function of the energy. The fusion excitation function of $^{36}S + ^{64}Ni$ was originally measured [22] several years ago, but fusion cross sections were determined down to about only $\sigma \simeq 50\ \mu b$. We have extended the measured cross section range to lower energies and a preliminary analysis of the present experiment was reported in Ref. [23].

In this article, the setup and the results are presented in the following section, while calculations within the CC model using a Wood-Saxon potential are described in Sec. III. A comparison with the results obtained for $^{36}S + ^{48}Ca$, $^{48}Ca + ^{48}Ca$, and for other nearby systems is performed in Sec. IV. Section V concludes this work with a short summary.

II. EXPERIMENT AND RESULTS

The experiment was performed using the ^{36}S beams of the XTU Tandem accelerator of LNL in the energy range $E_{lab} \simeq 81$ to 130 MeV. The beam intensity was between 7 and 15 pnA, and the target was a ^{64}Ni evaporation (99.6% enriched in mass 64), 50 $\mu g/cm^2$ thick, on a 20 $\mu g/cm^2$ carbon backing. Evaporation residues (ER), emitted near 0°, were detected using the electrostatic deflector setup described in Ref. [21]. The ER angular distribution for $^{36}S + ^{64}Ni$ has been measured at $E_{lab} = 91.0$ MeV (the Akyüz-Winther [24] Coulomb barrier is 90.4 MeV) in the angular range $-10°$ to $+10°$ in steps of 1°. This distribution is shown in Fig. 1(a). Fusion-fission is negligible for the present system so fusion cross sections were derived from the normalized 0° ER yields integrated over the angular distribution and corrected for the transmission T of the electrostatic deflector ($T = 0.72$ derived from systematic measurements performed for similar systems). The absolute cross-section scale is estimated to be accurate within $\simeq \pm 7\%$.

The present fusion cross sections and the previous data for $^{36}S + ^{64}Ni$ are in fair agreement by applying a suitable normalization coefficient [see the Fig. 1(b)]. One cannot go beyond this qualitative comparison since the beam incident energy, in the older measurements, was not known with the present accuracy resulting from the recalibration of the XTU Tandem accelerator [25]. We will concentrate on the present data in this article.

The fusion cross sections of $^{36}S + ^{64}Ni$ are listed in Table I. The excitation function appears to decrease smoothly in the sub-barrier region. The fusion excitation function is plotted in Fig. 2(a), together with the CC calculations discussed in Sec. III.

Extracting fusion barrier distributions (BD) [26] from the data greatly helps in revealing the fusion dynamics in the vicinity of the barrier, since CC effects effectively split the unperturbed barrier into a manifold or a continuous distribution of barriers, whose structure depends on the type of couplings [27] involved. Figure 2(b) shows the BD for $^{36}S + ^{64}Ni$ obtained by means of a double differentiation of $E\sigma_{fus}$ vs. energy using the three-point difference formula [26] with an energy step $\Delta E \simeq 2$ MeV. At first glance the BD shows only one main peak without a complex structure, as it is the case for stiff systems. However, the distribution is unusually wide (4–5 MeV). This indicates that it might be composed

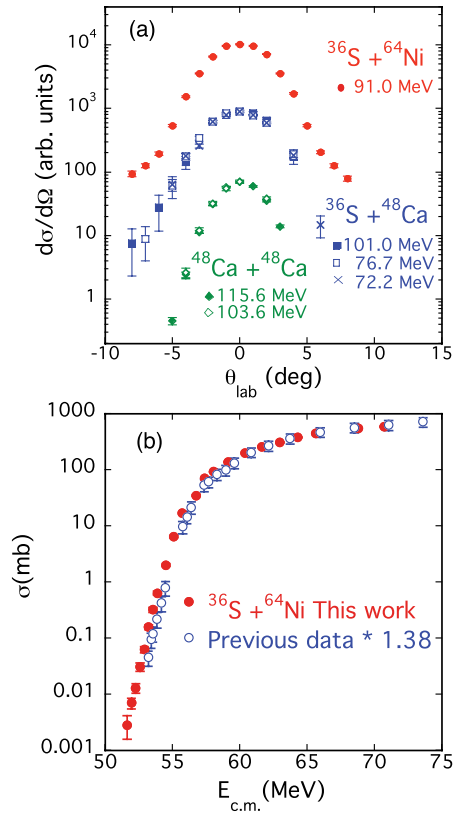

FIG. 1. (Color online) (a) ER angular distributions for $^{36}S + ^{64}Ni$, $^{36}S + ^{48}Ca$, and $^{48}Ca + ^{48}Ca$. (b) Fusion excitation function of $^{36}S + ^{64}Ni$. Previous data reported in Ref. [22] (open circles) have been normalized to the present results in the energy region above the barrier.

of various unresolved peaks originating from the low-lying quadrupole vibration in ^{64}Ni (see Sec. III).

The lowest-measured energy (corresponding to $\sigma \simeq 2.8\ \mu b$) is well below the threshold for hindrance E_{thr}^{emp}, predicted by the phenomenological systematics [28] (see Table II). In fact, one knows that hindrance usually shows up at an energy lower than E_{thr}^{emp} (see, e.g., Ref. [20]). This point will

TABLE I. Fusion cross sections of $^{36}S + ^{64}Ni$. Quoted errors are statistical uncertainties only.

$E_{c.m.}$ (MeV)	σ_{ER} (mb)	$E_{c.m.}$ (MeV)	σ_{ER} (mb)
51.63	0.0028 ± 0.0013	57.39	71.56 ± 2.09
51.95	0.0070 ± 0.0016	58.03	92.48 ± 2.05
52.27	0.013 ± 0.002	59.12	139.1 ± 2.8
52.59	0.031 ± 0.005	60.40	201.0 ± 4.4
52.91	0.063 ± 0.008	61.61	259.4 ± 3.9
53.23	0.158 ± 0.016	62.96	312.0 ± 5.9
53.55	0.323 ± 0.032	64.30	379.7 ± 6.3
53.87	0.639 ± 0.055	65.64	446.5 ± 3.9
54.51	2.01 ± 0.12	68.78	548.3 ± 9.6
55.08	6.41 ± 0.29	70.70	590.3 ± 8.9
55.72	17.14 ± 0.43	76.46	672.4 ± 13.3
56.75	35.06 ± 1.22	82.86	788.9 ± 35.9

TABLE II. Lowest measured energy E_{min}, and the corresponding cross section σ_{min} compared with the threshold energy E_{thr}^{emp} as estimated in Ref. [28], with the lower limit of the barrier distribution E_{BD}, and with the threshold indicated by CC calculations E_{cc} (see text).

System	E_{min} (MeV)	σ_{min} (μb)	E_{BD} (MeV)	E_{thr}^{emp} (MeV)	E_{cc} (MeV)
$^{36}S + ^{64}Ni$	51.63	2.86 ± 1.28	$\approx$53	55.11	$\simeq$54.5
$^{36}S + ^{48}Ca$	36.87	0.62 ± 0.35	$\approx$39	41.06	$\simeq$40.5
$^{48}Ca + ^{48}Ca$	46.35	0.58 ± 0.39	$\approx$48	51.46	$\simeq$48.3

be discussed in more detail in Sec. IV, where a comparison is done with the systems $^{36}S + ^{48}Ca$ and $^{48}Ca + ^{48}Ca$.

We know that fusion hindrance is expected to show up below the low-energy limit of the BD, where CC effects effectively vanish. With some degree of arbitrariness, we can identify this lower limit with the energy where the BD reduces to 0.01 MeV^{-1} (see the recent work on $^{58}Ni + ^{54}Fe$ [6]). This reference point is listed in the fourth column of Table II, and we notice that it is $\approx$2 MeV lower than the threshold energy of the systematics [20,28].

We have also examined the logarithmic slope $L(E)$ of the excitation function, which is a more effective way [1] of analyzing its behavior at very low energies. Figure 3(a) shows the experimental $L(E)$ values and the dashed line is the slope L_{CS} for a constant astrophysical S factor. The behavior of $^{36}S + ^{64}Ni$ ($Q = -8.5$ MeV) differs from that of heavier systems such as the Ni + Ni (with $Q < 0$) where the slope $L(E)$ crosses L_{CS} [2,4], corresponding to a maximum of the S factor. The slope of $^{36}S + ^{64}Ni$ has a steep increase around the barrier and approaches L_{CS} at low energies, but

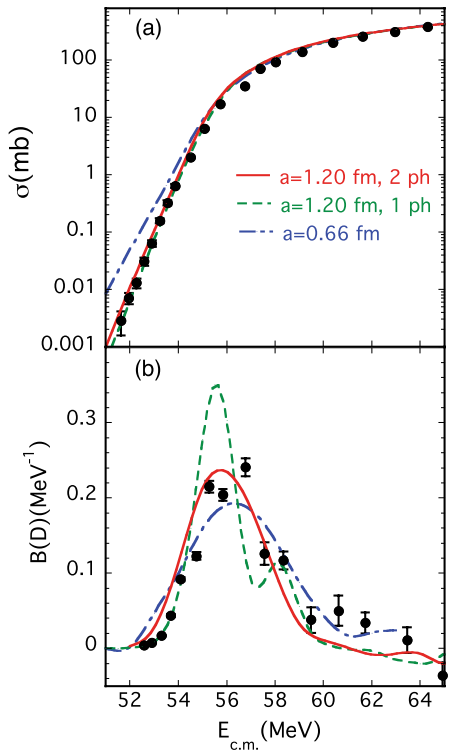

FIG. 2. (Color online) (a) The fusion excitation functions of $^{36}S + ^{64}Ni$ is compared with conventional CC calculations. (b) The experimental and theoretical barrier distributions are shown.

then a saturation shows up. This differs from what is shown in Ref. [23], where the result came from a preliminary data analysis. In Fig. 3 there is no clear evidence for a maximum of $S(E)$, and we are faced with the question whether fusion hindrance is observed in $^{36}S + ^{64}Ni$. We try to give an answer in the next section by comparing with CC calculations.

III. COUPLED-CHANNELS ANALYSIS

We have compared the measured cross sections with standard CC calculations performed with the CCFULL [29] code where the Woods-Saxon geometry for the nuclear potential is used. The Akyüz-Winther potential [24] (AW) and the low-lying collective states of target and projectile have been the starting point of our calculations. Excitation energies, spin and parities, and deformation parameters of these states are listed in Table III. The AW parameters have been slightly modified (essentially the depth V_o) to match the centroid of the experimental BD with the couplings included. The resulting potential is identified as "AW" in Table IV, with a barrier height 0.4 MeV higher than with the original AW parameters. One-phonon 2^+ and 3^- vibrations of projectile and target were included in the calculations as well as all possible mutual excitations. Since the quadrupole state of ^{64}Ni is rather strong, two-phonon excitations of this kind were included too. The calculated cross sections are compared with experimental data in Fig. 2 (see the dot-dashed line). A good fit is obtained near the barrier, but the data are strongly overpredicted below $\approx$54.5 MeV, i.e., slightly below the threshold energy for fusion hindrance expected from the systematics (fifth column of Table II). The energy where the BD vanishes is not far away (see again Table II).

In order to fit the data at low energies it is necessary to change drastically the potential parameters. Keeping the requirement to reproduce the centroid of the BD and using the same coupling scheme as mentioned above, the diffuseness

TABLE III. Excitation energies E_x, spin and parities λ^π, and deformation parameters β_λ [30,31] (see text) of states included in CC calculations.

Nucleus	E_x (MeV)	λ^π	β_λ
^{36}S	3.291	2^+	0.16
	4.192	3^-	0.38
^{48}Ca	3.832	2^+	0.11
	4.507	3^-	0.23
^{64}Ni	1.346	2^+	0.18
	3.560	3^-	0.20

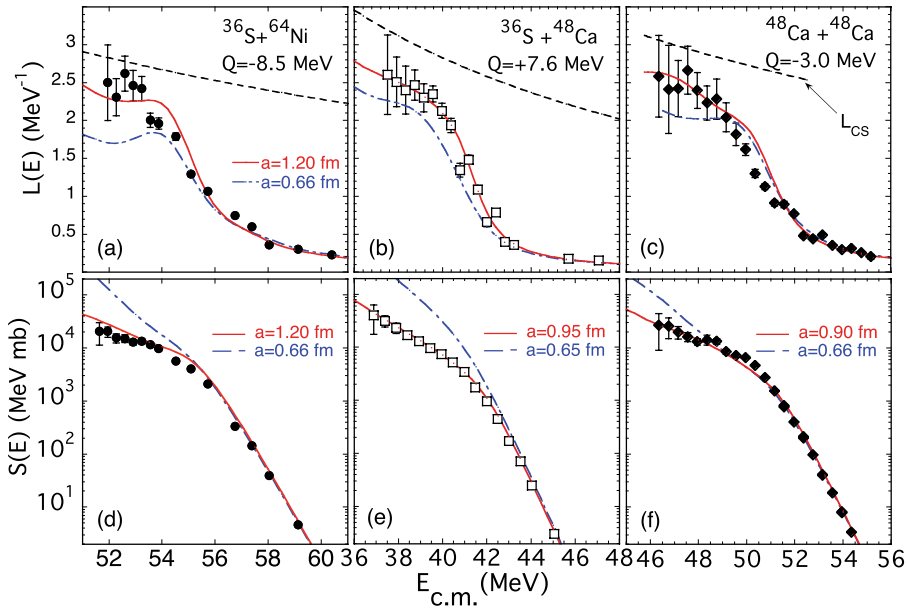

FIG. 3. (Color online) Logarithmic derivatives (a), (b), and (c) and S factors for three systems (d), (e), and (f) in comparison with CC calculations (see text). The results for ^{36}S + ^{48}Ca and ^{48}Ca + ^{48}Ca were already reported in Refs. [12,21]. We refer to those articles also for a detailed description of the CC calculations.

parameter has been varied in the CC calculations, until a reasonable agreement with the data was found. The radius parameter r_o and the depth V_o have been adjusted consequently. The results are shown in Fig. 2 (solid and dashed lines) and the new potential parameters are listed in Table IV (second line). A very large diffuseness parameter is needed (around $a = 1.2$ fm), and the difference between the results with one and two quadrupole phonons of ^{64}Ni is not so significant in the excitation function. However, reproducing the overall shape of the BD requires two-phonon couplings, since the calculation with only one phonon yields a BD which is too narrow with respect to the data. Additionally, the calculated two-peak structure is not clearly seen in the experimental BD. In spite of the large experimental errors at the lowest energies, the calculation with $a = 1.2$ fm reproduces fairly well the trend of $L(E)$ and of the S factor (see Fig. 3), although it seems to overestimate the slope around $\simeq$54–55 MeV.

All this indicates the presence of a suppression of fusion probability. It is actually known that the WS potential is generally not able to reproduce the low-energy fusion cross sections, with the standard AW parameters [24]. As a matter of fact, the very large diffuseness used here produces a broadening of the potential barrier (see the curvatures $\hbar\omega$ in Table IV), thus simulating a shallow potential, whose physical interpretation has been proposed in a recent theoretical model [13,14] of the hindrance phenomenon. Therefore, a detail search for the "best" diffuseness has little importance in the context of the present article.

IV. COMPARING WITH NEARBY SYSTEMS

The fusion of the two systems ^{36}S + ^{48}Ca and ^{48}Ca + ^{48}Ca was studied at LNL in recent years down to very small cross sections [12,21]. Figure 1 shows the experimental ER angular distributions for these two cases, and we give in Tables V and VI the measured cross sections which were not reported numerically in the original articles. The two excitation functions are very similar to each other. They are plotted in Fig. 4 together with the fusion barrier distributions extracted from the data in a similar way as for ^{36}S + ^{64}Ni (see above). The analogous behavior of ^{36}S, ^{48}Ca + ^{48}Ca is highlighted in the representation of the logarithmic derivative (slope) versus energy, shown in Fig. 3. The two slopes, after a sharp increase just below the Coulomb barrier, saturate with decreasing energy, even if the experimental uncertainties are large in the low-energy range. The slopes remain below the L_{CS} value, and, consequently, no maximum of the S factor shows up. The early hypothesis that the slope saturation may be due to the positive Q value of ^{36}S + ^{48}Ca has been contradicted by the parallel trend observed for ^{48}Ca + ^{48}Ca. The saturated slope is

TABLE IV. Parameters of the modified Akyüz-Winther potential [24] (see text) and those employed in our CC calculations, together with resulting barrier heights, radii, and curvatures.

System	Potential	V_o (MeV)	r_o (fm)	a (fm)	V_b (MeV)	r_b (fm)	$\hbar\omega$ (MeV)
^{36}S + ^{64}Ni	"AW"	58.0	1.18	0.66	58.5	10.27	3.47
	CC	208.1	0.80	1.2	58.5	9.59	2.65
^{36}S + ^{48}Ca	"AW"	65.8	1.15	0.65	43.3	9.90	3.35
	CC	164.6	0.90	0.95	43.3	9.54	2.82
^{48}Ca + ^{48}Ca	"AW"	54.7	1.18	0.66	52.2	10.27	3.23
	CC	84.9	1.05	0.90	51.9	10.03	2.76

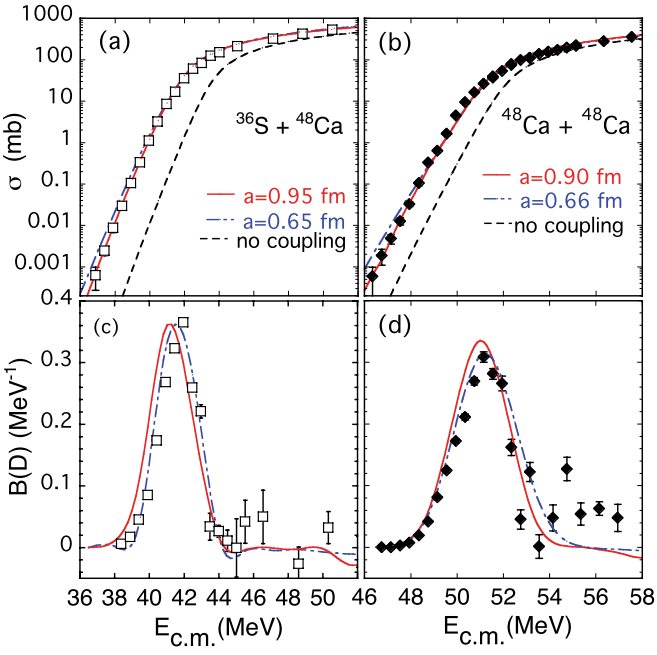

FIG. 4. (Color online) Fusion excitation functions of (a) $^{36}S + ^{48}Ca$ and (b) $^{48}Ca + ^{48}Ca$ recently measured at LNL. Cross sections are reported with only statistical uncertainties. Barrier distributions derived from the excitation functions are shown in panels (c) and (d).

not very different from the case of $^{36}S + ^{64}Ni$, however, nearby systems like various Ni + Ni cases [8,9] and the recently measured $^{58}Ni + ^{54}Fe$ system [6] display a totally different behavior.

In this respect, it is interesting to compare in more detail $^{36}S + ^{64}Ni$ with $^{36}S + ^{48}Ca$ and $^{64}Ni + ^{64}Ni$ [9] (each member of this "triplet" has one of the two colliding nuclei in common with another member). We show in Fig. 5 the logarithmic slopes versus the experimental fusion cross sections. This representation is only useful to compare the various systems with one another in the same frame, by eliminating trivial Coulomb barrier differences.

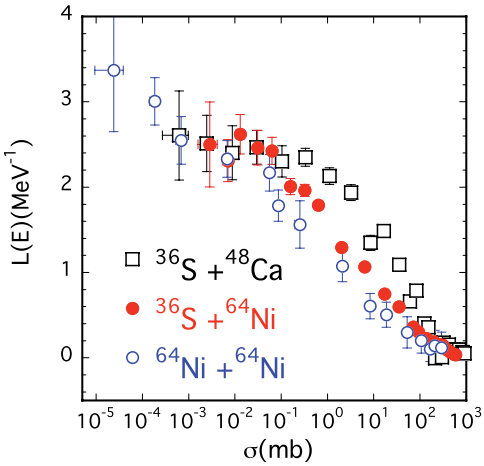

FIG. 5. (Color online) Logarithmic slopes versus experimental fusion cross sections for the three indicated systems.

TABLE V. Fusion excitation function of $^{36}S + ^{48}Ca$.

$E_{c.m.}$ (MeV)	σ_{ER} (mb)	$E_{c.m.}$ (MeV)	σ_{ER} (mb)
36.87	0.00062 ± 0.00035	43.52	124.6 ± 3.1
37.39	0.0025 ± 0.0006	44.02	150.9 ± 3.9
37.90	0.0088 ± 0.0020	45.05	213.3 ± 5.2
38.41	0.0296 ± 0.0042	47.10	323.1 ± 8.2
38.93	0.104 ± 0.014	48.82	423.1 ± 7.7
39.44	0.333 ± 0.025	50.53	533.4 ± 7.2
39.95	1.107 ± 0.077	52.24	612.2 ± 9.7
40.46	3.232 ± 0.219	53.96	699.0 ± 13.4
40.97	8.571 ± 0.538	55.67	799.6 ± 14.8
41.47	16.61 ± 0.76	57.39	840.4 ± 14.7
41.99	35.47 ± 1.48	59.10	915.2 ± 11.3
42.50	60.79 ± 2.56	60.81	972.7 ± 12.1
43.00	83.83 ± 2.20		

There is a recognizable trend when going from $^{36}S + ^{48}Ca$ to $^{36}S + ^{64}Ni$, and to $^{64}Ni + ^{64}Ni$, i.e., the slope increases less sharply between ≈100 mb to 0.1 mb (i.e., near and slightly below the barrier). This is probably a consequence of the increasing softness of the systems, leading to wider barrier distributions. At cross sections smaller than 0.1 mb the experimental errors are rather large, nevertheless a saturation shows up for the two lighter systems. The "plateau" between ≃1 and 100 μb appears to be a common feature of medium-light systems (see also $^{48}Ca + ^{48}Ca$), while only a hint of saturation may be inferred for $^{64}Ni + ^{64}Ni$.

One may argue that extending the measurement of fusion of $^{36}S + ^{48}Ca$ and $^{36}S + ^{64}Ni$ to lower energies the slope $L(E)$ would resume increasing, finally crossing L_{CS} and producing a maximum of the S factor. Indeed, the two lowest-energy points of $^{64}Ni + ^{64}Ni$ are crucial to establish the trend at far sub-barrier energies. Such measurements in the 10- to 100-nb region are obviously very difficult but badly needed in order to clear up the low-energy fusion dynamics.

The solid lines in Figs. 3 and 4 are the results of the CC calculations performed for $^{36}S + ^{48}Ca$ and $^{48}Ca + ^{48}Ca$, which were described in detail in the original articles [12,21].

TABLE VI. Fusion excitation function of $^{48}Ca + ^{48}Ca$.

$E_{c.m.}$ (MeV)	σ_{ER} (mb)	$E_{c.m.}$ (MeV)	σ_{ER} (mb)
46.35	0.00058 ± 0.00039	51.95	53.35 ± 0.88
46.75	0.0019 ± 0.0008	52.35	77.97 ± 1.65
47.15	0.0048 ± 0.0012	52.75	97.48 ± 1.10
47.55	0.0127 ± 0.0025	53.15	111.8 ± 2.2
47.95	0.0327 ± 0.0044	53.55	136.6 ± 1.1
48.35	0.105 ± 0.015	53.95	151.7 ± 2.8
48.75	0.328 ± 0.040	54.35	172.7 ± 1.5
49.15	0.569 ± 0.057	54.75	194.5 ± 1.8
49.55	1.28 ± 0.12	55.15	220.7 ± 3.9
49.95	4.48 ± 0.20	56.35	276.2 ± 3.7
50.35	9.35 ± 0.29	57.55	354.4 ± 5.3
50.75	16.12 ± 0.37	58.75	409.4 ± 6.4
51.15	26.12 ± 0.56	60.75	505.5 ± 5.6
51.55	36.62 ± 0.93		

They follow the same philosophy reported for $^{36}S + ^{64}Ni$ in this work. Tables III and IV list the properties of low-energy quadrupole and octupole vibrations included in the CC calculations, and the parameters of the WS ion-ion potentials, respectively, for each system. The diffuseness parameter needed to fit the low-energy data, is substantially larger for $^{36}S + ^{64}Ni$ ($a \simeq 1.2$ fm) with respect to the other two systems ($a = 0.90$–0.95 fm). Qualitatively, this can be appreciated from Figs. 2 and 4, where the deviation of the experimental excitation function of $^{36}S + ^{64}Ni$ from the CC predictions using the AW potential starts at larger cross sections and is much more clear-cut than observed for ^{36}S, $^{48}Ca + ^{48}Ca$.

Only with very large diffuseness parameters it is possible to reproduce the low-energy part of the excitation functions, and this indicates the presence of the hindrance phenomenon. When comparing (Table II) the energies E_{cc} below which the CC calculations fail to reproduce the data with the ones, E_{BD}, at which the BD essentially goes to zero, one can note that these values are lower than the threshold energies for hindrance indicated by systematics (E_{thr}^{emp}), as qualitatively expected. It has been suggested [20] that a high neutron excess might push fusion hindrance to lower energies. Indeed, $^{36}S + ^{64}Ni$ is a neutron-rich system with $N - Z = 12$. This does not differ very much from the cases of ^{36}S, $^{48}Ca + ^{48}Ca$, where $N - Z = 12$ and 16, respectively. Very recently, the system $^{40}Ca + ^{48}Ca$ (with a smaller neutron excess) has been investigated [32] and an S-factor maximum was observed without any slope saturation.

The barrier distributions of ^{36}S, $^{48}Ca + ^{48}Ca$ are shown in Figs. 4(c) and 4(d) respectively. Both systems are very stiff, and one main peak dominates the distribution. However, a second small peak on the right of the main one may be identified in $^{48}Ca + ^{48}Ca$ [see Fig. 4(d)]. This second peak remains unexplained within the CC calculations performed here, and its possible cause has been the subject of a recent work [33].

V. SUMMARY

New data on sub-barrier fusion of $^{36}S + ^{64}Ni$ have been presented. The fusion excitation function has been extended to cross sections around 3 μb well below the expected threshold for fusion hindrance. The BD has been extracted from the data; most of the strength is in a wide peak near the nominal barrier, probably originating from couplings to the low-lying quadrupole vibrations in ^{64}Ni. Standard CC calculations using the AW potential overestimate the data already close to the barrier. The low-energy part of the excitation function can be reproduced only using a very large diffuseness for the WS potential. This can be regarded as evidence of fusion hindrance. The low-energy limit of the BD and the energy where the measured cross sections fall below the standard CC calculations are lightly lower (1–2 MeV) than the threshold energy for hindrance indicated as an upper limit by the systematics.

The logarithmic derivative $L(E)$ of the excitation function, which is sensitive to its detailed behavior at very low energies, has been examined. With decreasing energies below the barrier, it saturates slightly below the L_{CS} value, in analogy with the cases of ^{36}S and $^{48}Ca + ^{48}Ca$. We can qualitatively argue that nuclear structure (coupling) effects are still active down to the lowest measured energies, so observing the crossing of $L(E)$ with L_{CS} requires extending the experiments to still lower energies.

A detailed comparison of the three systems $^{36}S + ^{64}Ni$, $^{36}S + ^{48}Ca$, and $^{64}Ni + ^{64}Ni$ strengthens this indication, since the trend of $L(E)$ for $^{36}S + ^{64}Ni$ at very low energies differs from $^{64}Ni + ^{64}Ni$ (or from $^{58}Ni + ^{54}Fe$ and $^{58}Ni + ^{58}Ni$) because the slope keeps increasing below the barrier above L_{CS} in these heavier systems, and no (intermediate) saturation shows up. The reason why this is so, appears to be connected to different nuclear structure situations, but it is awaiting a quantitative theoretical explanation.

ACKNOWLEDGMENTS

Grateful thanks are due to the XTU Tandem staff for their effort to ensure good beam quality and fast energy changes. This work was partially supported by the European Commission within the 6th Framework Programme through I3-EURONS (Contract No. RII3-CT-2004-506065).

[1] C. L. Jiang *et al.*, Phys. Rev. Lett. **89**, 052701 (2002).
[2] C. L. Jiang, B. B. Back, H. Esbensen, R. V. F. Janssens, and K. E. Rehm, Phys. Rev. C **73**, 014613 (2006).
[3] C. L. Jiang, B. B. Back, R. V. F. Janssens, and K. E. Rehm, Phys. Rev. C **75**, 057604 (2007).
[4] C. L. Jiang, H. Esbensen, B. B. Back, R. V. F. Janssens, and K. E. Rehm, Phys. Rev. C **69**, 014604 (2004).
[5] M. Dasgupta, D. J. Hinde, A. Diaz-Torres, B. Bouriquet, Catherine I. Low, G. J. Milburn, and J. O. Newton, Phys. Rev. Lett. **99**, 192701 (2007).
[6] A. M. Stefanini *et al.*, Phys. Rev. C **82**, 014614 (2010).
[7] E. M. Burbridge, G. R. Burbridge, W. A. Fowler, and F. Hoyle, Rev. Mod. Phys. **29**, 547 (1957).
[8] M. Beckerman, J. Ball, H. Enge, M. Salomaa, A. Sperduto, S. Gazes, A. DiRienzo, and J. D. Molitoris, Phys. Rev. C **23**, 1581 (1981).
[9] C. L. Jiang *et al.*, Phys. Rev. Lett. **93**, 012701 (2004).
[10] C. L. Jiang *et al.*, Phys. Lett. B **640**, 18 (2006).
[11] C. L. Jiang, Proc. Int. Conf. on "New Aspects of Heavy Ion Collisions Near the Coulomb Barrier," Fusion08, Chicago, IL, 22–26 September 2008, AIP Conf. Proc. 1098, edited by K. E. Rehm, B. B. Back, H. Esbensen, and C. J. Lister (AIP, Melville, NY, 2009), p. 145.
[12] A. M. Stefanini *et al.*, Phys. Lett. B **679**, 95 (2009).
[13] Ş. Mişicu and H. Esbensen, Phys. Rev. Lett. **96**, 112701 (2006).
[14] Ş. Mişicu and H. Esbensen, Phys. Rev. C **75**, 034606 (2007).
[15] C. H. Dasso and G. Pollarolo, Phys. Rev. C **68**, 054604 (2003).
[16] T. Ichikawa, K. Hagino, and A. Iwamoto, Phys. Rev. C **75**, 057603 (2007).
[17] T. Ichikawa, K. Hagino, and A. Iwamoto, Phys. Rev. Lett. **103**, 202701 (2009).

[18] A. Diaz-Torres, D. J. Hinde, M. Dasgupta, G. J. Milburn, and J. A. Tostevin, Phys. Rev. C **78**, 064604 (2008).
[19] C. L. Jiang *et al.*, Phys. Rev. C **78**, 017601 (2008).
[20] C. L. Jiang *et al.*, Phys. Rev. C **81**, 024611 (2010).
[21] A. M. Stefanini *et al.*, Phys. Rev. C **78**, 044607 (2008).
[22] A. M. Stefanini *et al.*, Nucl. Phys. A **456**, 509 (1986).
[23] A. M. Stefanini, in Ref. [11], p. 3.
[24] Ö. Akyüz and Å. Winther, in *Nuclear Structure and Heavy Ion Physics*, Proc. Int. School of Physics "Enrico Fermi," Course LXXVII, Varenna, edited by R. A. Broglia and R. A. Ricci (North Holland, Amsterdam, 1981).
[25] D. Ackermann *et al.*, Laboratori Nazionali di Legnaro Annual Report 1993, p. 258.
[26] N. Rowley, G. R. Satchler, and P. H. Stelson, Phys. Lett. B **254**, 25 (1991).
[27] M. Dasgupta, D. J. Hinde, N. Rowley, and A. M. Stefanini, Annu. Rev. Nucl. Part. Sci. **48**, 401 (1998).
[28] C. L. Jiang, K. E. Rehm, B. B. Back, and R. V. F. Janssens, Phys. Rev. C **79**, 044601 (2009).
[29] K. Hagino, N. Rowley, and A. T. Kruppa, Comput. Phys. Commun. **123**, 143 (1999).
[30] S. Raman, C. W. Nestor, Jr., and P. Tikkanen, At. Data Nucl. Data Tables **78**, 1 (2001).
[31] T. Kibédi and R. H. Spear, At. Data Nucl. Data Tables **80**, 35 (2002).
[32] C. L. Jiang *et al.*, Phys. Rev. C **82**, 041601(R) (2010).
[33] N. Rowley and K. Hagino, Nucl. Phys. A **834**, 110c (2010).